Advanced MR techniques in brain tumor imaging

Sasan Karimi, MD; Nicole M. Petrovich, BA; Kyung K. Peck, PhD; Bob L. Hou, PhD; Andrei I. Holodny, MD

The imaging of brain tumors has significantly improved with the use of advanced magnetic resonance (MR) techniques, such as spectroscopy, perfusion, and functional imaging. Conventional MR imaging (MRI) provides mainly anatomic or structural information about the brain. Unlike conventional imaging, advanced MR techniques also provide physiological information concerning metabolism and hemodynamics. These techniques not only aid in the imaging diagnosis of brain tumors, they may also play a role in clinical management of patients with brain tumors. A concise compendium of the physiology, techniques, and clinical applications of MR perfusion imaging, spectroscopy, functional MR imaging (fMRI), and diffusion tensor imaging (DTI) in the setting of neuro-oncology is reviewed in this article.

Perfusion imaging

Brain tumors can induce angiogenesis or the formation of new blood vessels. Hypoxia, which occurs as a tumor outgrows its blood supply, can produce angiogenic cytokines; these cytokines are responsible for angiogenesis.[1] Tumor vessels that are produced in this manner are histologically abnormal and more permeable than normal. They are also disorganized and tortuous.[2] These vascular abnormalities and altered flow dynamics lead to changes in blood volume and flow, which are exploited in MR perfusion imaging. The most frequently used measure of perfusion in neuro-oncology is the cerebral blood volume (CBV). The cerebral blood volume (or the volume of blood passing through a portion of the brain) is measured in milliliters of blood per 100 grams of brain tissue (mL/100 g).

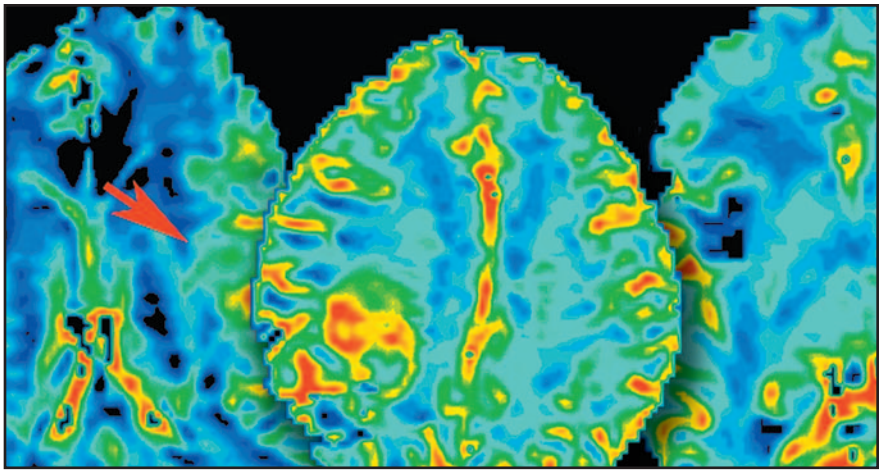

The most common perfusion technique is T2* dynamic susceptibility imaging. The T2* effects of gadolinium result in decreased signal intensity during the passage of gadolinium. The change in signal intensity is plotted against time to form a signal intensity time curve (Figure 1). The CBV is estimated from the area encompassed by the curve, which is inverted in this case, since there is signal loss. Repetitive imaging is performed shortly before, during, and after the passage of gadolinium. Generally, 0.2 mmol/Kg of gadolinium is injected at a high rate using a power injector. The CBV is normalized to uninvolved portions of the brain. In cases in which an arterial input function is not determined, only a relative CBV (rCBV) can be calculated. Dynamic susceptibility perfusion imaging is based on the premise that contrast material remains within the intravascular compartment. High permeability or leakiness in regions of marked breakdown of the blood-brain barrier (BBB) results in intravascular gadolinium extravasating into the interstitial space. Extravasation can significantly affect calculations and alter CBV values. Several methods have been used to correct—or, more appropriately, compensate for—the unwanted effect of extravasation on rCBV calculations, including excluding portions of the signal intensity time curve from the calculations. This corrective method still leads to underestimation of the rCBV.

Dr. Karimi *is an Assistant Professor, Department of Radiology,* ***Ms. Petrovich*** *is the Senior Neurodiagnostic fMRI Specialist, Department of Radiology,* ***Dr. Peck*** *is an Instructor, and* ***Dr. Hou*** *is an Assistant Attending Physician, Department of Medical Physics, and* ***Dr. Holodny*** *is a Professor, Department of Radiology, Memorial Sloan-Kettering Cancer Center, New York, NY.*

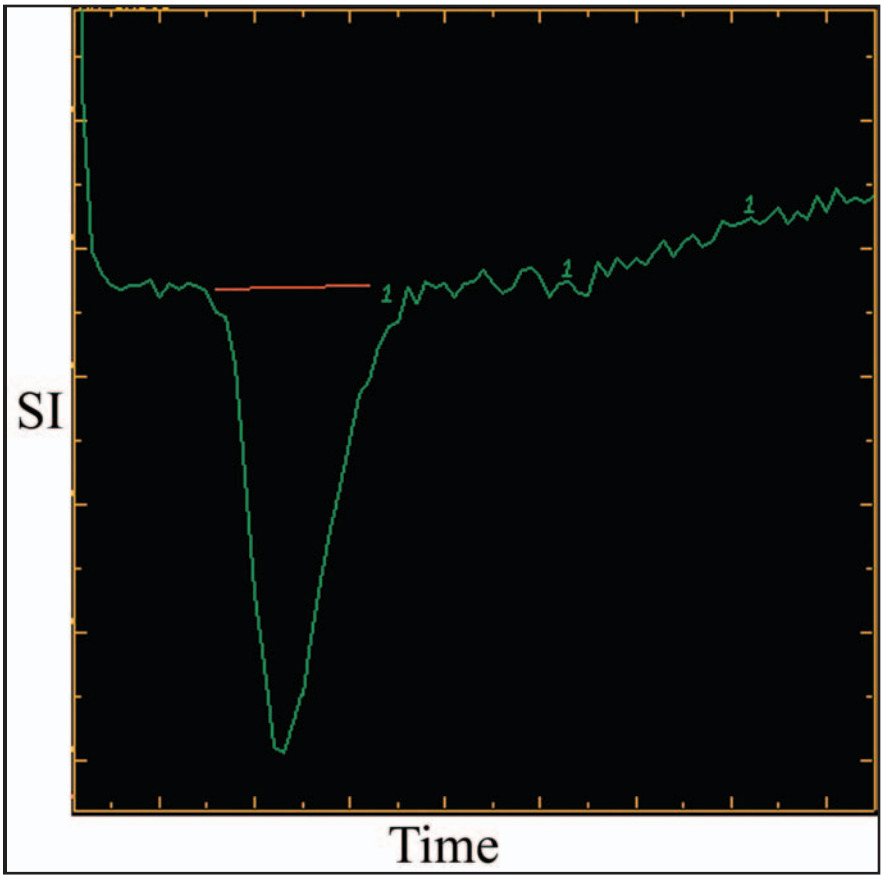

FIGURE 1. *This signal intensity [SI] time curve shows a decrease in SI as gadolinium passes through.*

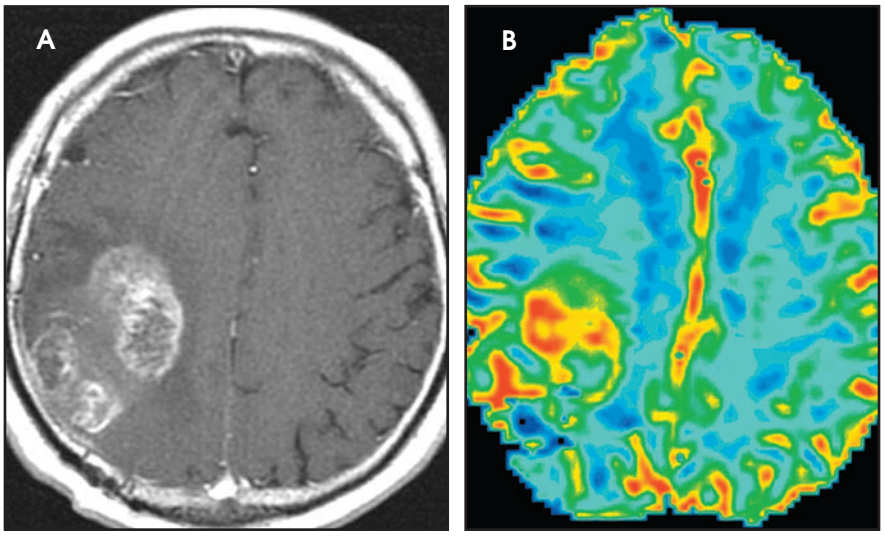

FIGURE 2. *Biopsy-proven glioblastoma multiforme. (A) An axial T1-weighted postcontrast MR image shows a heterogeneous enhancing lesion within the posterior right frontal and parietal lobes. (B) Increased blood volume in the region of the tumor is shown on the relative cerebral blood volume map.*

Another method, sloping baseline, leads to artifactually high rCBV. Using T1-weighted dynamic perfusion imaging can eliminate the problem with the breakdown of the BBB and permeability. In this technique, tumor enhancement or permeability itself is used to calculate the rCBV, so it does not need to be corrected.[3]

In general, high-grade brain tumors have greater rCBV than low-grade lesions (Figure 2).[1,2,4,5] MR perfusion can help identify and localize higher grade components of tumors in guiding stereotactic biopsy and can also provide a noninvasive estimate of tumor grade (Figure 3).[1-4] Since the enhancing or even the T2 borders of gliomas do not represent the true margins of the tumor, MR perfusion can be more sensitive in defining the true extent of gliomas than can anatomic MR imaging.[6] Better delineation of tumor borders can help in radiation and surgical planning. In the future, MR perfusion imaging will probably play a role in better defining tumor margins for radiation and surgical planning.

Differentiating tumor recurrence from radiation necrosis is a problem that clinicians and radiologists face frequently. It should be noted that cases of pure tumor recurrence and radiation necrosis occur in only a minority of cases. The majority of cases fall within a spectrum containing a mixture of both tumor and necrosis. This adds further complexity to reaching a correct diagnosis. Unlike tumors, which have elevated rCBV, radiation necrosis has been shown to have diminished rCBV (Figure 4).[7] Since a significant number of patients fall within the spectrum, perfusion imaging is of limited value in differentiating between the two. The advantage of MR perfusion CBV data is its high positive predictive value for the presence of high-grade malignancy. In other words, if the CBV maps reveal elevated perfusion, there is tumor present. The specificity of the diagnostic task can be increased when perfusion imaging is combined with MR spectroscopy.

Measurements of rCBV have been shown to be more useful in assessing response to radiotherapy in patients treated with stereotactic radiosurgery (SRS).[8] The vascularity of metastases can decrease within a few weeks of treatment; however, the volume of enhancement might not change for several months. MR perfusion imaging seems

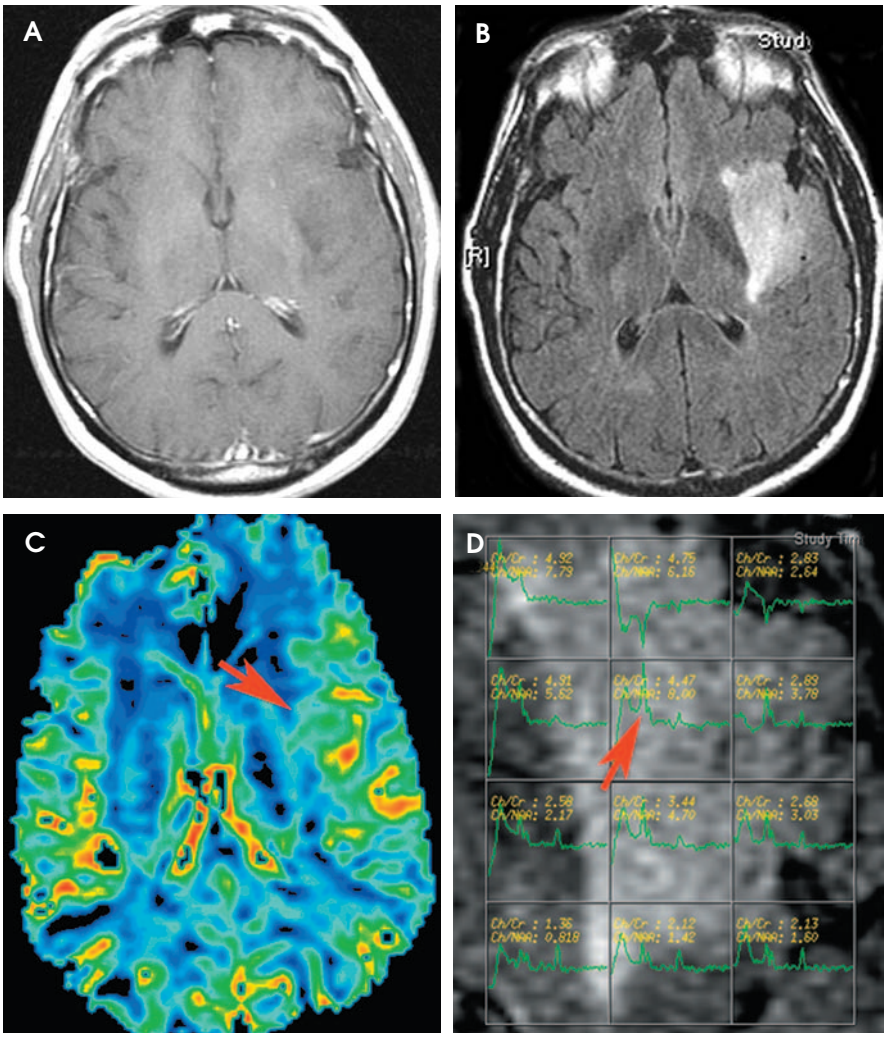

FIGURE 3. *(A) The axial T1-weighted postgadolinium image is unremarkable, with no evidence of abnormal enhancement. (B) An axial fluid-attenuated inversion recovery image at the same levels as in (A) shows abnormal hyperintensity in the left peri-insular region, which is suggestive of a low-grade primary tumor, given its lack of enhancement. (C) The relative cerebral blood volume map shows a subtle asymmetric increase in blood volume in the left subinsular region (arrow), which suggests a high-grade tumor. (D) The marked elevation of the choline-to-creatine ratio (arrow) is also suggestive of a high-grade tumor. A biopsy of the lesion confirmed that it was a high-grade tumor, an anaplastic astrocytoma.*

promising in the follow-up of patients with brain metastasis, but more research is necessary to evaluate its potential.

Spectroscopy

Clinical applications of proton magnetic resonance spectroscopy (1H-MRS) are increasing as the techniques and hardware have become more robust and user-friendly. Proton MRS provides biochemical and metabolic information about tumors and normal brain.[9] The information obtained from 1H-MRS is unique and independent of that obtained from other MRI techniques. In their study of pediatric brain tumors, Tzika et al[10] showed that there is no correlation between the metabolic profile of tumors and other imaging parameters, such as enhancement, diffusion, and rCBV.

Spectroscopy can be done in single- or multivoxel (MRS imaging) forms. The 2 most commonly used methods for volume selection/excitation are stimulated echo acquisition mode (STEAM) and point-resolved spectroscopy sequence (PRESS). In general, shorter echo times are better achieved with STEAM; however, it is more sensitive to motion.[11] In theory, for the same total echo time, the signal of PRESS is twice as great as that of STEAM; PRESS is also less sensitive to motion. With improving software, PRESS seems to be the most commonly used method of volume selection in clinical practice at present time.

The advantage of single-voxel 1H-MRS is its short acquisition time (approximately 5 minutes). The down side is that it lacks spatial resolution and cannot be used to better define the true extent of a glioma. Histologically, gliomas are heterogeneous, and, therefore, single-voxel spectroscopy cannot be used to map regional metabolic variation. In other words, single-voxel spectroscopy alone cannot reliably define the highest-grade components of the tumor. It may also suffer from significant averaging with adjacent normal brain tissues.

In the spectroscopy literature, the most commonly used echo times are 144 msec and 270 msec. At these long echo times, the spectrum is dominated by 5 different metabolite peaks. These are the choline (Cho)-containing compounds, creatine (Cr), N-acetylaspartate (NAA), lactate, and lipid (Figure 5). The choline peak reflects cell membrane turnover. Creatine is a good surrogate for energy synthesis, and NAA is a marker that is exclusive to neuronal cells. Lactate results from anaerobic metabolism and is detected in necrotic tumors and infarcted tissue. Cellular and myelin breakdown products result in prominent lipid peaks. In tumors, choline-containing compounds are increased, and NAA is decreased relative to uninvolved or normal brain tissue.[12,13] This pattern of metabolic change is the spectroscopic hallmark of brain tumors.

Combined with MRI, MRS can aid in the evaluation of tumor type and grade. The higher-grade gliomas tend to exhibit higher Cho/Cr and Cho/NAA ratios. The high-grade gliomas also tend to have lipid and lactate as the result of necrosis (Figure 6).[14] MR spectroscopy can help differentiate enhancing tumor from other causes of enhancement (mainly necrosis) and is more specific in differentiating nonenhancing tumor from edema and

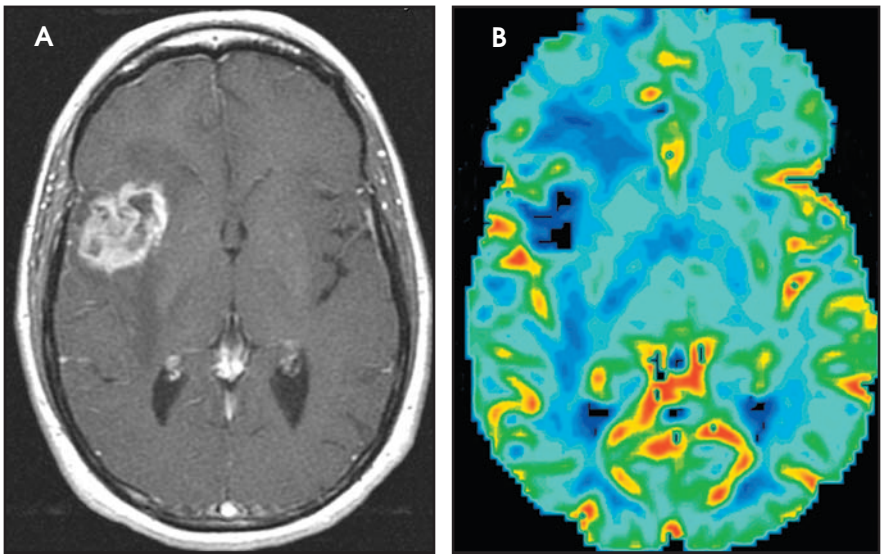

FIGURE 4. *(A) An axial T1-weighted MR image of a patient with renal cell carcinoma who was treated with stereotactic radiosurgery for a brain metastasis. The heterogeneous enhancing right insular metastasis was slightly larger following radiotherapy. (B) The relative cerebral blood volume map shows marked decreased blood volume in the region of enhancement, which is consistent with radiation necrosis as the dominant underlying cause of enhancement. The lesion has been stable on subsequent follow-up examinations.*

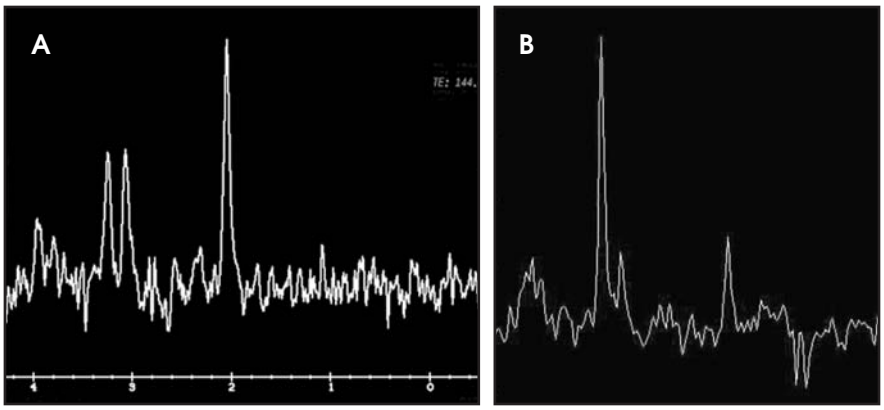

FIGURE 5. *(A) A single-voxel spectrum of normal brain shows the choline-to-creatine (Cho/Cr) ratio near unity. (B) A single-voxel spectrum of a glioblastoma multiforme reveals a marked increase in the Cho/Cr ratio, decreased N-acetylaspartate, and a lactate doublet, which is inverted at long echo time (144 msec).*

other causes of T2 prolongation. These qualities have been exploited in order to better define the true extent and morphology of gliomas. This information has the potential to significantly alter target volumes and doses in radiation therapy of brain gliomas when compared with conventional radiotherapy. Although this is an attractive concept, there are no studies to show benefits, changes in failure patterns, or improved survival. MR spectroscopy is utilized more and more by different groups in assessing response to therapy in patients with primary brain tumors or metastases.

MR spectroscopy can noninvasively enable the distinction between a solitary metastasis and high-grade gliomas, particularly when combined with perfusion MR imaging. In their study, Law et al[15] showed that measurements of Cho and mean rCBV in the perienhancing region are useful in differentiating solitary metastases from high-grade gliomas. In the perienhancing region, T2 prolongation is partly due to tumor infiltration (nonenhancing tumor) in patients with high-grade gliomas. Whereas in the case of metastases, the hyperintensity surrounding the region of enhancement is due to vasogenic edema or nonspecific treatment effects rather than infiltrating tumor. Therefore, elevated levels of choline and/or rCBV surrounding a peripherally enhancing mass reflect tumor infiltration in a high-grade glioma (Figure 7).

As with perfusion MRI, MRS is also useful in estimating tumor grade. It is commonly observed that the Cho/Cr ratio increases with histologic grade.[16,17] However, because of the innate heterogeneity of brain tumors, there is a significant overlap between Cho/Cr levels and tumor grade.

Following treatment, MRS has a limited role in the assessment of patients. Frequently, there is a mixture of tumor and necrosis after therapy. This limits the utility of MRS in differentiating residual/recurrent tumor from radiation necrosis, as is the case with MR perfusion. As a tumor responds to treatment, the choline decreases and lactate and/or lipids may increase.[18,19] MR spectroscopy can play a useful role after treatment in assessing the therapeutic response. This is particularly important for early detection of treatment failure so that an ineffective treatment can be modified prior to a significant progression of disease.

Functional MRI

Functional MRI is used for the purpose of neurosurgical planning and neurologic risk assessment in the treatment of brain tumors.[20,21] It localizes the eloquent cortices controlling language, motor, and memory functions. The results of an fMRI study can alter a neurosurgical approach to a tumor, suggest that surgery is a safe option in cases in which it might not otherwise have been offered, or steer a clinician away from neurosurgery and toward other treatment options when the risk of damage to the eloquent cortex is high.

Functional MRI is commonly used to map language function.[23-25] It is used to localize the areas of the cortex working to support speech and to determine hemispheric dominance for language

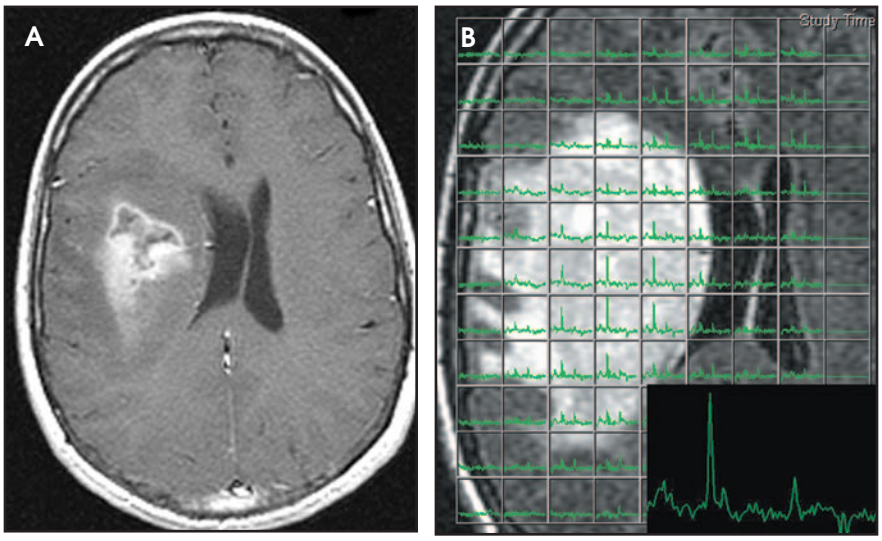

FIGURE 6. *A biopsy-proven glioblastoma multiforme. (A) An axial T1-weighted MR image shows an infiltrative enhancing mass within the right frontal lobe with central necrosis. (B) An MR spectroscopic image overlaid on an axial fluid-attenuated inversion recovery image that encompasses the tumor and surrounding brain tissue is consistent with a necrotic high-grade tumor (magnified representative voxel—lower right-hand corner).*

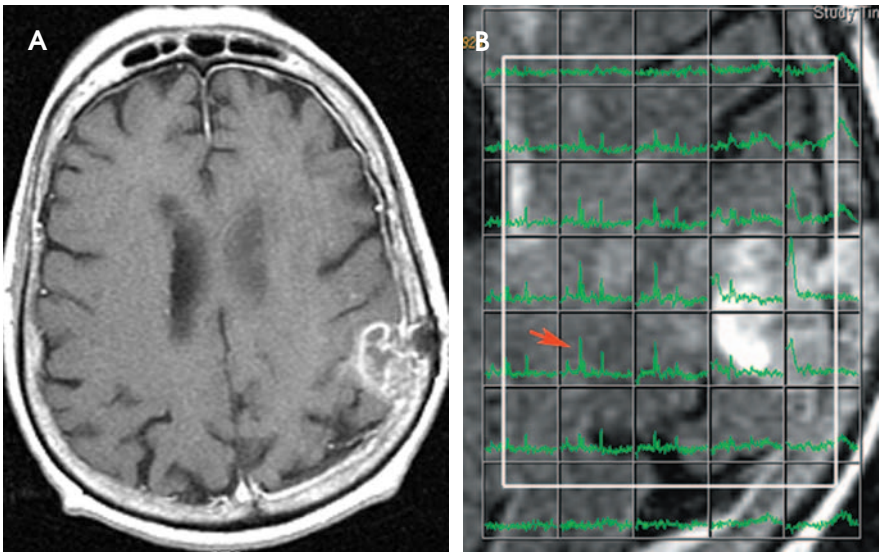

FIGURE 7. *(A) An axial postcontrast T1-weighted MR image shows a heterogeneous mass in the left parietal lobe. (B) A "screen save" from a 3-dimensional MR spectroscopic image is overlaid onto a magnified fluid-attenuated inversion recovery (FLAIR) scout image, showing an increased choline-to-creatine ratio in the perienhancing region. Note the relative lack of abnormal FLAIR hyperintensity in the perienhancing region (arrow).*

(Figure 8). Because fMRI is based on a noninvasive, endogenous signal, it has the potential to replace the invasive Wada test (also known as the intracarotid amytal test), which is the current gold standard in language and memory lateralization.[26,27]

Functional MRI has revealed unexpected hemispheric language dominance in both adults and children.[28-30] In a case described by our group,[28] a 62-year-old right-handed man with a mostly nonenhancing left temporoparietal glioma in the expected anatomic location of Wenicke's area presented without language impairment. The fMRI revealed split hemispheric dominance for language, with Broca's area localizing to the left hemisphere and Wernicke's to the right hemisphere. Intraoperative electrocortical stimulation confirmed the fMRI results, and the patient underwent gross-total resection. This patient might not otherwise have been offered an operation had the fMRI not suggested atypical language localization.

Language paradigms vary with the location of the tumor. Typically, for frontal lesions, the patient will perform tasks such as generating words to a presented letter or verbs to visually presented nouns, punctuated by periods of rest. For posterior language localization, patients can be asked to name pictures or fill in the appropriate missing word in a sentence. While targeted testing is preferable, often both Broca's and Wernicke's areas are activated during both productive and receptive language tasks, making it not essential to tailor the language task to the lesion location. However, it should be noted that posterior language function (Wernicke's area), like many cognitive tasks, can be difficult to measure in patients.[31] A targeted approach may help lessen the variability in capturing this sometimes elusive language area.

The Wada test produces information about both language and memory function. As a result, the ability to use fMRI to noninvasively measure both language and memory function may further displace the Wada test. There is as yet no commonly accepted set of memory tasks for the purpose of neurosurgical planning. Golby et al[32] use a "novel versus repeated" protocol through which verbal memory and spatial memory can be measured. In this protocol, the patient is presented with novel and repeated images of faces, patterns, scenes, and word pairs (in separate trials). The analysis yields those areas that are active during the novel trials in which the patient encodes the new stimuli. As noninvasive, repeatable techniques, such as fMRI, improve in the measurement of hemispheric dominance for memory and language, invasive tests, with their associated morbidity (such as the Wada test), will be replaced.

FIGURE 8. *A preoperative blood-oxygen-level–dependent functional MRI performed with language task shows Broca's (green arrow) and Wernecke's (yellow arrow) areas.*

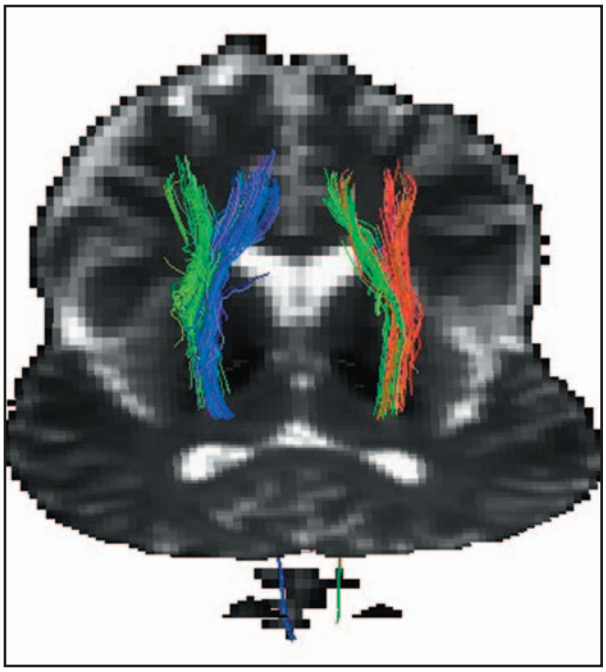

FIGURE 10. *A diffusion tractography image in a normal volunteer shows the corticospinal tracts of the hand and the foot bilaterally extending from the precentral gyrus (the location of the motor homunculus) to the posterior limb of the internal capsule.*

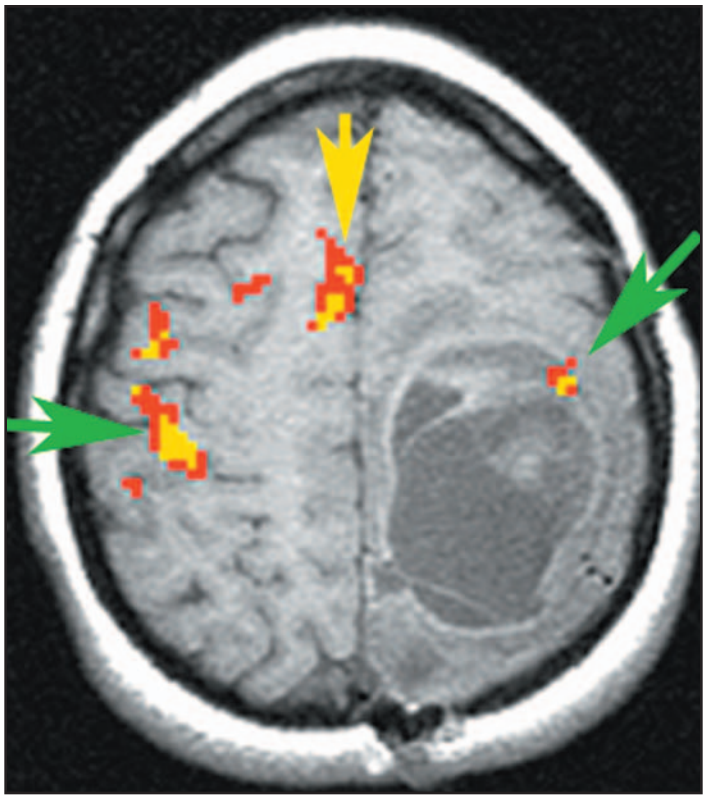

FIGURE 9. *A preoperative blood-oxygen-level–dependent functional MRI with a bilateral finger-tapping paradigm shows the spatial relationship between the tumor and motor activation (green arrow), contralateral motor activation (green arrow), and supplemental motor activation (yellow arrow). Note the relative decrease in activation on the side of the tumor.*

Motor mapping, by contrast, is relatively easy for cognitively impaired patients to perform and produces consistent and reliable fMRI maps.[33] Often, patients perform cued movements of the fingers, feet, and/or tongue, depending on the location of the lesion (Figure 9).

Localizing the motor strip and coregistering the results to a surgical scan prior to a neurosurgical intervention can help guide the direct cortical stimulation during an awake craniotomy and possibly shorten operation time. In some cases, using fMRI to confirm the expected location of the motor strip may avoid awake neurosurgery altogether.

Diffusion tensor imaging: A way to see beyond the gray areas

Although blood-oxygen-level–dependent (BOLD) fMRI is able to directly visualize the exact location of a functional area of the brain adjacent to a brain tumor,[34,35] there is a limitation in that the technique can depict activation only in the cortical gray matter. Therefore, the information provided to the operating neurosurgeon is limited to the cortex. Brain tumors also invade the white matter,[36,37] however, BOLD fMRI is not able to provide accurate information about the location of major white matter tracts. Accidental resection or transection of a major white matter tract can lead to devastating consequences.

There are 2 main reasons why preoperative identification of white matter tracts is important. First, accurate localization of important white matter tracts can affect the decision of whether or not to operate.

For example, if the main mass of the tumor straddles the corticospinal tract, a neurosurgeon may be averse to even attempting a gross total resection. Clearly, knowledge of the location of the corticospinal tract in such a case would be advantageous, since the neurosurgeon would not have to perform a craniotomy, operate on the brain, and perform direct white matter stimulation only to discover that the tumor is inoperable. Secondly, preoperative localization of important white matter tracts is essential in surgical planning. For example, in a tumor that involves the corona radiata, it is often very difficult, if not impossible, to determine the relationship of the tumor to the corticospinal tract or the thalamocortical tract. This task becomes even more difficult with the inevitable presence of mass effect and infiltration of normal structures by tumor. Consequently, the neurosurgeon may assume that the majority of the tumor to be resected is anterior to the corticospinal tract, only to discover during the operation that in reality, the corticospinal tract is posterior to the tumor and that the initial approach taken has been incorrect.

Diffusion tensor imaging[38,39] is a new MRI technique that is sensitive to directional movements of water molecules and that allows the identification of functional white matter tracts in vivo. Diffusion tensor imaging has the potential to establish spatial relationships between eloquent white matter and tumor borders and provide clinically valuable information to assess the progression and regression of white matter tracts as a result of tumor growth or resection.

In gray matter, it is usually sufficient to characterize the diffusion characteristics with a single apparent diffusion coefficient (ADC), because measured water diffusivity is largely independent of the orientation of the tissue. However, in an anisotropic area, such as white matter, where the measured diffusivity is known to depend upon the orientation of the tissue, a single ADC is not able to describe the orientation-dependent water mobility in the tissue. Diffusion tensor imaging, which is based on the orientation-dependent water diffusion, can be achieved using a single-shot diffusion-weighted (DW) spin-echo echo-planar imaging (EPI) pulse sequence, in which 2 symmetric trapezoidal gradient pulses are added around a 180° refocusing pulse in the required gradient channel. Sets of DW-EPI images are collected with diffusion gradients applied sequentially along at least 6 predetermined directions. From the DTI data, the 6 independent elements of the diffusion tensor can be calculated for each pixel. In tensor theory,[38] the directions of the main axes represent the so-called eigenvectors and their length the so-called eigenvalues of the tensor. Diagonalization of the tensor can be used to calculate the eigenvalues (λ_1,λ_2,λ_3) and the eigenvector. The vector corresponding to the largest eigenvalue represents the direction in which water diffusion is greatest and is assumed to correspond to the predominant fiber orientation within each voxel. The elements of the tensor are used to yield a mean diffusivity map (D) and the fractional anisotropy (FA). *D* is an indicator of free water fraction. *FA* is used to measure the fraction of the total magnitude of *D* that is anisotropic and has a value of 0 for isotropic diffusion ($\lambda_1=\lambda_2=\lambda_3$) and 1 for complete anisotropic diffusion ($\lambda_1>0$; $\lambda_2=\lambda_3=0$). Therefore, it describes deviation from isotropic diffusion. Previous studies[37,40] have shown that neoplasms and surrounding edematous brain have an increase of free water fraction (high *D* value) and loss of structural organization (reduced *FA* value).

A number of recent developments have led to a new application of DWI termed *diffusion tractography*. This application uses diffusion tensor data to identify specific white matter tracts as opposed to white matter tracts in general (Figure 10). For example, one can determine the location of the corticospinal tract or the thalamocortical tract and differentiate these tracts from all other white matter tracts in the corona radiata. The ability to exactly define specific tracts traversing the corona radiata and other nebulous white matter structures has already had an impact on the treatment of brain lesions. A number of recent publications have shown remarkable images of specific white matter tracts in normal subjects using diffusion tractography.[41,42] However, this technology has just made its appearance and will no doubt expand even further.

Conclusion

The integration of advanced imaging techniques (such as fMRI, spectroscopy, DTI, and perfusion imaging) will offer increasingly detailed information about pathologic processes. Furthermore, it is hoped that such detailed information will aid in the development of new treatments and will improve our understanding of the mechanism underlying neurological disorders.

References

1. Jackson A, Kassner A, Annesley-Williams D, et al. Abnormalities in the recirculation phase of contrast agent bolus passage in cerebral gliomas: Comparison with relative blood volume and tumor grade. *AJNR Am J Neuroradiol.* 2002;23:7-14.
2. Provenzale JM, Wang GR, Brenner T, et al. Comparison of permeability in high-grade and low-grade brain tumors using dynamic susceptibility contrast MR imaging. *AJR Am J Roentgenol.* 2002;178:711–716.
3. Covarrubias DJ, Rosen BR, Lev MH. Dynamic magnetic resonance perfusion imaging of brain tumors. *Oncologist.* 2004;9:528-537.
4. Lev MH, Rosen BR. Clinical applications of intracranial perfusion MR imaging. *Neuroimaging Clin N Am.* 1999;9:309-331.
5. Roberts HC, Roberts TP, Brasch RC, Dillon WP. Quantitative measurement of microvascular permeability in human brain tumors achieved using dynamic contrast-enhanced MR imaging: Correlation with histologic grade. *AJNR Am J Neuroradiol.* 2000;21:891-899.
6. Henry RG, Vigneron DB, Fischbein NJ, et al. Comparison of relative cerebral blood volume and proton spectroscopy in patients with treated gliomas. *AJNR Am J Neuroradiol.* 2000;21:357-366.
7. Aronen HJ, Perkio J. Dynamic susceptibility contrast MRI of gliomas. *Neuroimaging Clin N Am.* 2002;12: 501-523.
8. Essig M, Waschkies M, Wenz F, et al. Assessment of brain metastases with dynamic susceptibility-weighted contrast-enhanced MR imaging: Initial results. *Radiology.* 2003;228:193-199.
9. Howe FA, Opstad KS. 1H MR spectroscopy of brain tumours and masses. *NMR Biomed.* 2003;16: 123-131.
10. Tzika AA, Zarifi MK, Goumnerova L, et al. Neuroimaging in pediatric brain tumors: Gd-DTPA-enhanced, hemodynamic, and diffusion MR imaging compared with MR spectroscopic imaging. *AJNR Am J Neuroradiol.* 2002;23:233-333.
11. Castillo M, Kwock L, Mukherji SK. Clinical applications of proton MR spectroscopy. *AJNR Am J Neuroradiol.* 1996;17(1):1-15.
12. Usenius JP, Kauppinen RA, Vaino PA, et al. Quantitative metabolite patterns of human brain tumors: Detection by 1H NMR spectroscopy in vivo and in vitro. *J Comput Assist Tomogr.* 1994;18:705-713.

13. Usenius JP, Vainio P, Hernesniemi J, et al. Choline-containing compounds in human astrocytomas studied by 1H NMR spectroscopy in vivo and in vitro. *J Neurochem.* 1994;63:1538-1543.
14. Nelson SJ. Multivoxel magnetic resonance spectroscopy of brain tumors. *Mol Cancer Ther.* 2003;2: 497-507.
15. Law M, Cha S, Knopp EA, et al. High-grade gliomas and solitary metastases: Differentiation by using perfusion and proton spectroscopic MR imaging. *Radiology.* 2002;222:715-721.
16. Howe FA, Barton SJ, Cudlip SA, et al. Metabolic profiles of human brain tumors using quantitative in vivo 1H magnetic resonance spectroscopy. *Magn Reson Med.* 2003;49:223-232.
17. Gill SS, Thomas DG, Van Bruggen N, et al. Proton MR spectroscopy of intracranial tumours: In vivo and in vitro studies. *J Comput Assist Tomogr.* 1990;14: 497-504.
18. Shino A, Nakasu S, Matsuda M, et al. Noninvasive evaluation for the malignant potential of intracranial meningiomas performed using proton magnetic resonance spectroscopy. *J Neurosurg.* 1999;91: 928-934.
19. Graves EE, Nelson SJ, Vigneron DB, et al. Serial proton MR spectroscopic imaging of recurrent malignant gliomas after gamma knife radiosurgery. *AJNR Am J Neuroradiol.* 2001;22:613-624.
20. Vlieger EJ, Majoie CB, Leenstra S, Den Heeten GJ. Functional magnetic resonance imaging for neurosurgical planning in neuroncology. *Eur Radiol.* 2004; 14:1143-1153.
21. Wilkinson ID, Romanowski CA, Jellinek DA, et al. Motor functional MRI for pre-operative and intraoperative neurosurgical guidance. *Br J Radiol.* 2003;76: 98-103.
22. Moritz C, Haughton V. Functional MR imaging: Paradigms for clinical preoperative mapping. *Magn Reson Imaging Clin N Am.* 2003;11:529-542.
23. Huang J, Carr TH, Cao Y. Comparing cortical activations for silent and overt speech using event-related fMRI. *Hum Brain Mapp.* 2002;15(1):39-53.
24.Larner AJ, Robinson G, Kartsounis LD, et al. Clinical-anatomical correlation in a selective speech production impairment. *J Neurol Sci.* 2004;219:23-29.
25. Li P, Jin Z, Tan LH. Neural representations of nouns and verbs in Chinese: An fMRI study. *Neuroimage.* 2004;21:1533-1541.
26. Kho KH, Leijten FS, Rutten GJ, et al. Discrepant findings for Wada test and functional magnetic resonance imaging with regard to language function: Use of electrocortical stimulation mapping to confirm results. Case report. *J Neurosurg.* 2005;102:169-173.
27. Schulze-Bonhage A, Quiske A, Loddenkemper T, et al. Validity of language lateralisation by unilateral intracarotid Wada test. *J Neurol Neurosurg Psychiatry.* 2004;75:1367-1368.
28. Petrovich NM, Holodny AI, Brennan CW, Gutin PH. Isolated translocation of Wernicke's area to the right hemisphere in a 62-year-man with a temporo-parietal glioma. *AJNR Am J Neuroradiol.* 2004;25:130-133.
29. Holodny AI, Schulder M, Ybasco A, Liu WC. Translocation of Broca's area to the contralateral hemisphere as the result of the growth of a left inferior frontal glioma. *J Comput Assist Tomogr.* 2002;26: 941-943.
30. Derakhshan I. Unsuspected atypical hemispheric dominance for language as determined by FMRI. Handedness: Neural versus behavioral: The difference is measurable. *Epilepsia.* 2003;44:734-735.
31. Price CJ, Veltman DJ, Ashburner J, et al. The critical relationship between the timing of stimulus presentation and data acquisition in blocked designs with fMRI. *Neuroimage.* 1999;10(1):36-44.
32. Golby AJ, Poldrack RA, Brewer JB, et al. Material-specific lateralization in the medial temporal lobe and prefrontal cortex during memory encoding. *Brain.* 2001;124(Pt 9):1841-1854.
33. Rutten GJ, Ramsey N, Noordmans HJ, et al. Toward functional neuronavigation: Implementation of functional magnetic resonance imaging data in a surgical guidance system for intraoperative identification of motor and language cortices. Technical note and illustrative case. *Neurosurg Focus.* 2003;15(1):E6.
34. Bogomolny DL, Petrovich NM, Hou BL, et al. Functional MRI in the brain tumor patient. *Top Magn Reson Imaging.* 2004;15:325-335.
35. Haberg A, Kvistad KA, Unsgard G, Haraldseth O. Preoperative blood oxygen level-dependent functional magnetic resonance imaging in patients with primary brain tumors: Clinical application and outcome. *Neurosurgery.* 2004;54:902-914.
36. Nimsky C, Ganslandt O, Hastreiter P, et al. Intraoperative diffusion-tensor MR imaging: Shifting of white matter tracts during neurosurgical procedures—initial experience. *Radiology.* 2005; 234:218-225.
37. Sinha S, Bastin ME, Whittle IR, Wardlaw JM. Diffusion tensor MR imaging of high-grade cerebral gliomas. *AJNR Am J Neuroradiol.* 2002;23:520-527.
38. Basser PJ, Jones DK. Diffusion-tensor MRI: Theory, experimental design and data analysis—a technical review. *NMR Biomed.* 2002;15:456-467.
39. Le Bihan D, Mangin JF, Poupon C, et al. Diffusion tensor imaging: Concepts and applications. *J Magn Reson Imaging.* 2001;13:534-546.
40. Tropine A, Vucurevic G, Delani P, et al. Contribution of diffusion tensor imaging to delineation of gliomas and glioblastomas. *J Magn Reson Imaging.* 2004;20:905-912.
41. Holodny AI, Gor DM, Watts R, et al. Diffusion-tensor MR tractography of somatotopic organization of corticospinal tracts in the internal capsule: Initial anatomic results in contradistinction to prior reports. *Radiology.* 2005;234:649-653.
42. Conturo TE, Lori NF, Cull TS, et al. Tracking neuronal fiber pathways in the living human brain. *Proc Natl Acad Sci USA.* 1999;96:10422-10427.